Impact of Spark Assistance and Multiple Injections on Gasoline PPC Light Load

Jesús Benajes, Bernardo Tormos, Antonio García and Javier Monsalve-Serrano
Universitat Politècnica de València

Abstract

Along the last years, engine researchers are more and more focusing their efforts on the advanced low temperature combustion (LTC) concepts with the aim of achieving the stringent limits of the current emission legislations. In this regard, several studies based on highly premixed combustion concepts such as HCCI has been confirmed as a promising way to decrease drastically the most relevant CI diesel engine-out emissions, NOx and soot. However, the major HCCI drawbacks are the narrow load range, bounded by either misfiring (low load, low speed) or hardware limitations (higher load, higher speeds) and the combustion control (cycle-to-cylce control and combustion phasing). Although several techniques have been widely investigated in order to overcome these drawbacks, the high chemical reactivity of the diesel fuel remains as the main limitation for the combustion control.

The attempts of the researchers to overcome these disadvantages are shifting to the use of fuels with different reactivity. In this sense, gasoline PPC has been able to reduce emissions and improve efficiency simultaneously, but some drawbacks regarding controllability and stability at low load operating conditions still need solution. In this field, previous researches have been demonstrate the multiple injection strategy as an appropriate technique to enhance the combustion stability. However, PPC combustion has been found limited to engine loads higher than 5 bar BMEP when using fuels with octane number greater than 90. In this regard, previous work from the authors showed the capability of the spark plug to provide combustion control in engine loads below this limit even using 98 ON gasoline.

The main objective of the present work is to couple the control capability of the spark assistance together with an appropriate mixture distribution by using double injection strategies with the aim of evaluating performance and engine-out emissions at low load PPC range using a high octane number gasoline. For this purpose the optical and metal version of a compression ignition single-cylinder engine, to allow high compression ratio, has been used during the research. A common rail injection system enabling high injection pressures has been utilized to supply the 98 octane number gasoline. An analysis of the in-cylinder pressure signal derived parameters, hydroxyl radical (OH*) and natural luminosity images acquired from the transparent engine as well as a detailed analysis of the air/fuel mixing process by means of a 1-D in-house developed spray model (DICOM) has been conducted. Results from both analysis methods, suggest the spark assistance as a proper technique to improve the spatial and temporal control over the low load gasoline PPC combustion process. A noticeable increase in the cycle to cycle repeatability (5% versus 15.1% CoV IMEP at 2 bar load) as well as a reduction in the knocking level (20.5 versus 33.6 MW/m^2 at 7 bar load) is observed. In addition, the combination of the spark assistance with the use of the double injection strategy provides a great improvement in terms of combustion efficiency (93% versus 88% for a single injection strategy) with a benefit around 18% in the IMEP.

Introduction

The automotive scientific community and manufacturers are currently focusing part of their efforts on the investigation of new combustion modes [1,2] and on the optimization of the current technology with the aim of reducing fuel consumption and emissions in CI diesel engines [3]. Most of these new combustion concepts are achieved by using different strategies that produce a lean air-fuel mixture together with a low temperature combustion. It contributes to decrease drastically the most relevant CI diesel engine-out emissions, NOx and soot [4]. In addition, due to the in-cylinder mixture homogeneity, a fast heat release is obtained when the proper in-cylinder conditions are achieved providing high combustion efficiency.

These combustion concepts based on fully or partially premixed lean mixtures are commonly known as Homogeneous Charge Compression Ignition (HCCI) [5,6]. Even though they achieve important emission benefits [7], these combustion concepts present some practical issues that must be overcome before they can be implemented in CI diesel engines being confined to low engine speeds and loads [8]. The most relevant limitations of this combustion modes consist of achieving an appropriate combustion phasing, the cycle-to-cycle control of the combustion process, spray impingements and its effects on the emissions [9], the noise and operating range extent. Several techniques such as EGR [10], variable valve timing [11,12], variable compression ratio [13] and intake air temperature variation [14] have been investigated in order to overcome these drawbacks. Due to the high chemical reactivity of the diesel fuel, the mentioned techniques cannot provide precise control over the combustion

phasing since they require large time scales to achieve cycle-to-cycle control. Thus, not enough mixing time before the start of combustion is provided.

The scientific community is currently trying to overcome these disadvantages by using fuels with different reactivity [15-17]. In this sense, Partially Premixed Combustion (PPC) using a low reactivity fuel has been confirmed as promising method to control the heat release rate providing a reduction in NOx and soot emissions as well. The use of a high ON fuel, such as gasoline, in a CI engine under PPC conditions provides more flexibility to reach lean and low combustion temperatures due to the extra mixing time achieved [18] through the fuel properties. However, the concept has demonstrated difficulties at low load conditions using gasoline with octane number greater than 90, concluding that the use of a low reactivity fuel under PPC conditions provide some control on combustion phasing but still do not solve the possibility of cycle-to-cycle control. In order to mitigate the main drawbacks encountered when using single injection strategies at low load, several researchers investigated the use of multiple injection strategies, which improve the control over the fuel/air mixture preparation before SOC. Thus, some level of mixture stratification in the chamber has been shown necessary to improve low load operation. The double injection strategy provides sufficient mixing time before the SOC to achieve a homogeneous charge as well as the reactive conditions required to trigger the combustion process, improving the combustion stability. However, to achieve auto-ignition time scales small enough for combustion in the engine, an increase in the intake pressure and temperature is required [19]. Thus, multiple injection strategies have been found as a suitable method for improving the combustion stability but fuels with octane number greater than 90 do not allow to run PPC below 5 bar BMEP load.

Recent investigations on gasoline engines (SI) running in homogenous or premixed combustion modes such as CAI (always PFI) [20,21], have shown the potential of using the assistance of a spark plug for achieving cycle-to-cycle control and combustion phasing control. The results suggest that this strategy can provide good combustion phasing while the response time is short enough for cycle-to-cycle application. Nevertheless, further research on spark assistance in new combustion modes is necessary for continuing its development with low reactivity fuels [22,23].

Thus, with the aim of integrating phasing and cycle-to-cycle control by means of a spark plug ignition system in a CI engine working in partially premixed charge, the PPC concept with spark assistance fuelled with high ON gasoline has been studied. This engine architecture has a high compression ratio and it is equipped with a common rail injection system that enables high injection pressures. In addition, the impact of double injection strategies has been investigated. The present work focuses on couple the control capability of the spark assistance together with an appropriate mixture distribution by using double injection strategies with the aim of evaluating their impact on gasoline PPC performance and engine-out emissions using a high ON gasoline. For this purpose the optical and metal version of a compression ignition single-cylinder engine, to allow high compression ratio, has been used during the research. A common rail injection system enabling high injection pressures has been utilized to supply the 98 ON gasoline. An analysis of the in-cylinder pressure signal derived parameters, OH* and natural luminosity images acquired from the transparent engine as well as a detailed analysis of the air/fuel mixing process by means of a 1-D in-house developed spray model (DICOM) has been conducted.

Experimental Facilities and Processing Tools

Test cell

This section presents the experimental configuration of the test cell and the main subsystems used in this study. As Figure 1 shows, the single cylinder engine is installed in a fully instrumented test cell, with all the auxiliary facilities required for operation and control.

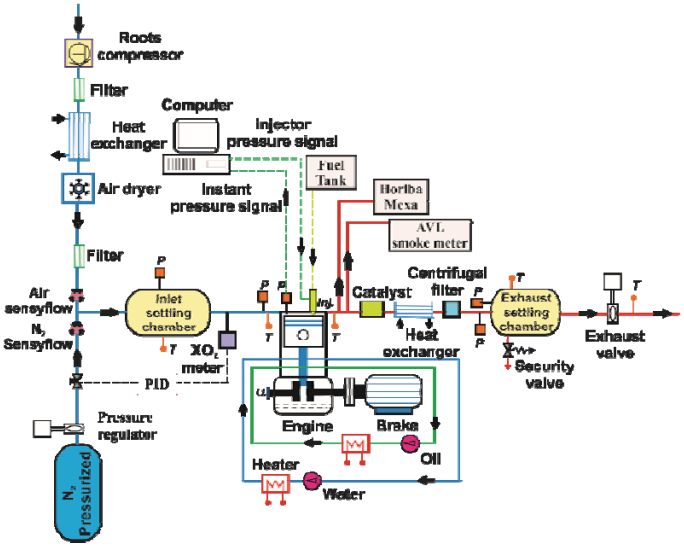

Figure 1. Complete test cell setup.

The intake air is supplied by a roots compressor with an upper pressure limit of 3 bar. Then, the air flows through a filter to remove possible impurities. The heat exchanger and the air dryer allow controlling the temperature and humidity of the intake air independently on the ambient conditions. The temperature in the inlet settling chamber is maintained constant by using a heater in the intake line. The oxygen concentration variation is performed using a synthetic EGR system. EGR is substituted by nitrogen gas, which greatly simplifies the system ensuring a controllable gas composition without an excessive time to adjust the facility. Despite the limited practical application, it was decided to use this method to have a better control of the variables, which allows studying the underlying phenomena more carefully. The concept is based on decreasing the O_2 concentration at the inlet manifold by increasing the flow of N_2 and keeping constant the total intake mass flow rate (substitution EGR). For this purpose a PID controller is equipped to operate the N_2 valve governed by the intake O_2 meter. With this system, the in-cylinder thermodynamic conditions can be reproduced systematically. To ensure a homogeneous mixture of N_2 and O_2 and to attenuate pressure pulses in the intake manifold, a settling chamber of 500 liters volume is used in the installation.

During the metal engine version tests, the exhaust gases were analyzed with a five gas Horiba MEXA 7100 D analyzer bench. In order to increase the robustness of these measurements, the different pollutant volume fractions were sampled and averaged over an 80 second time period after attaining steady state operation. CO and unburned HC measurements were used to determine the combustion efficiency (1):

$$Comb.Eff = \left(1 - \frac{HC}{mf} - \frac{CO}{4 \cdot mf}\right) \cdot 100 \quad (1)$$

Smoke emissions were measured with an AVL 415 variable sampling smoke meter, providing results directly in FSN. The FSN values used in this research are the average of three consecutive measurements at the same operating condition. These measurements were transformed into mg/m^3 by means of the correlation (2) proposed in the user manual of the device:

$$[mg/m^3] = \frac{1}{0.405} \cdot 4.95 \cdot FSN \cdot e^{0.38 \cdot FSN} \quad (2)$$

In the exhaust line, after the exhaust analyzer sample probe, a catalyst is mounted to prevent the accumulation of unburned hydrocarbons in the installation. Due to the low temperatures achieved during the combustion event and therefore in the exhaust line, the catalyst is often operating with low efficiency and a centrifugal filter is needed to remove the rest of the hydrocarbons. In the same way as in the intake line, a settling chamber is mounted in order to attenuate pressure pulses. Finally, an exhaust backpressure valve is equipped to maintain a relative pressure of 0.2 bar to the intake pressure, in order to simulate a representative air management conditions of a real turbocharged engine.

Engine configurations and cylinder head adaptation

Cylinder head adaptation

A spark plug is required to implement the partially premixed compression ignition with spark assistance combustion mode. As Figure 2 shows, the cylinder head has been modified by removing an exhaust valve and thus enabling the insertion of the spark plug in the combustion chamber. A standard spark plug (Veru Platinum) with a 1 mm gap is used along with a custom electronic control system. In the standard configuration, the tip protrudes 4.5 mm into the combustion chamber from the cylinder head plane and it is located 17 mm from the cylinder axis. The injector is centered and vertically assembled in the modified cylinder head with a graduated metal circle that can change the relative position between the spark plug and the injector fuel jets by rotating the injector around its vertical axis. This relative position is fixed to make the spray pass between the spark electrodes.

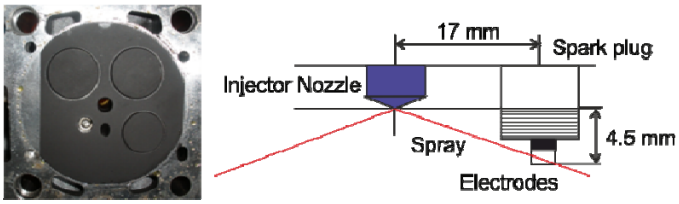

Figure 2. Image of the modified cylinder head with spark plug and injector hole (left). Diagram of the relative position between the injector and spark plug (right).

Metal engine configuration

The engine used in the present study is a 3-valve, 0.545 l displacement single cylinder engine with a modified cylinder head for the study of this combustion mode. The bowl dimensions are 45x18 mm (diameter x depth). Table 1 presents the main characteristics of the engine.

Table 1. Main characteristics of the single cylinder engine used in the present study.

Type	CI, 4stroke, DI
Max. engine speed	4500 rpm
Cylinder number	1
Displacement	544.75 cm^3
Bore	85 mm
Stroke	96 mm
Compression ratio	14.7:1
Bowl diameter	45 mm
Bowl depth	18 mm
Bowl volume	25 cm^3

In order to increase the reliability of the combustion mode, a Delphi multicharge ignition system [24,25] has been used. The high amount of energy released by this ignition system allows igniting the mixture even with local equivalence ratio conditions near their flammability limits with high EGR rates [24]. The spark ignition system is operated at a constant nominal primary voltage of 15 V from the battery and primary current of 25 A, providing around 120 mJ for the typical combustion chamber density test conditions, almost double than a conventional ignition system.

The fuel injection system is based on an electronically controlled Bosch common rail system. The injector is a Bosch piezoelectric CRIP 3.3 model equipped with a seven-hole nozzle with 154° included angle. The nozzle hole diameter is 97 microns and its flow capacity is 210 cm^3/30 s. The injection control system makes it possible to modify any parameter of the injection events such as the start of injection timing, injection duration and rail pressure. The fuel injection hardware characteristics are summarized in Table 2.

Table 2. Main characteristics of the injection system used in the present study.

Actuation Type	Piezoelectric
Steady flow rate @ 100 bar	210 cm^3/30s
Number of Holes	7
Hole diameter	97 µm
Included Spray Angle	154°

In order to characterize the most relevant properties of the gasoline used in this research, various analyses of the fuel properties have been performed following ASTM standards. It is worthy to note that 300 ppm of additive (Havoline Performance Plus) was added to improve the lubricity of the gasoline up to diesel fuel level, increasing the service life of the high pressure pump and fuel injector. The addition of the additive does not modify neither density nor the viscosity. The results of the gasoline characterization are summarized in Table 3.

Table 3. Main characteristics of the gasoline used in the present study.

Fuel	Gasoline
Density (T= 15°C)	722 kg/m^3
Viscosity (T= 40°C)	0.37 mm^2/s
Research octane number	98
Lower heating value	44542 kJ/kg

Optical engine configuration

The engine is equipped with an elongated piston with a cylindrical bowl, which allows optical access to the combustion chamber through a sapphire window placed in its bottom. Below the piston bowl, an elliptical UV mirror is placed on the cylinder axis. In front of the mirror, a beam splitter (50%-50%) is positioned in order to allow the simultaneous acquisition of the OH radical luminosity and the natural luminosity. For the acquisition of the natural luminosity images, a high speed Phantom V12 CMOS camera equipped with a 100 mm focal length Zeiss lens is utilized with an image resolution of 512 x 512 pixels. In order to acquire the OH radical luminosity images a Photron intensified camera equipped with a 100 mm UV lens together with a band pass filter centered at 310 nm is utilized. Figure 3 shows the optical scheme. It is interesting to note that the tests have been performed under skip-fired mode (1 cycle fired per 30) in order to avoid excessive thermal stress in the windows and ensure the same in-cylinder initial thermodynamic conditions for the recorded (fired) cycles. Due to the high dilution in the exhaust line, it is not possible to measure the engine-out emissions when the optical engine configuration is used. Thus, the fuel energy conversion efficiency (3) calculated from the rate of heat release not by means of the direct measurement of CO and unburned HC as done in when the metal engine version is used:

$$FeCE = \frac{100}{m_f \cdot LHV} \int_{IVC}^{EVO} RoHR(\alpha) \cdot d\alpha \quad (3)$$

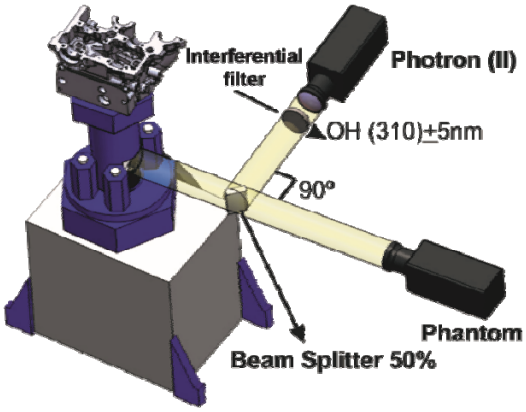

Figure 3. Optical scheme for the images acquisition during the combustion process. Natural luminosity (NL) and OH* radical.

Theoretical tools

Analysis of pressure signal

The combustion analysis is performed with an in-house developed one-zone model named CALMEC, which is fully described in [26]. This combustion diagnosis tool uses the in-cylinder pressure as its main input. The in-cylinder pressure was measured with a Kistler 6067C1 pressure transducer. A shaft encoder with 1800 pulses per revolution was used, which supplies a resolution of 0.2 CAD. The pressure traces for 200 engine cycles were recorded in order to compensate the cycle-to-cycle variation during engine operation. Thus, each individual cycle's pressure data was smoothed using a Fourier series low-pass filter. Once filtered, the collected cycles were ensemble averaged to yield a representative cylinder pressure trace, which was used to perform the analysis. Then, the first law of thermodynamics is applied between IVC and EVO, considering the combustion chamber as an open system because of blow-by and fuel injection. The ideal gas equation of state is used to calculate the mean gas temperature in the chamber. Along with these two basic equations, several sub-models are used to calculate instantaneous volume and heat transfer [27]. The main result of the model is the Rate of Heat Release (RoHR). Information related to each cycle can be obtained, such as the IMEP. Start of combustion (SoC) is defined as the crank angle position in which the RoHR slope begins to rise due to combustion and combustion phasing is defined as the crank angle position of 50% fuel mass fraction burned (CA50). Additionally, ringing intensity (4) is calculated by means of the correlation of Eng [28]:

$$RI = \frac{1}{2\gamma} \frac{[0.05 \cdot (dP/dt)_{max}]^2}{P_{max}} \sqrt{\gamma R T_{max}} \quad (4)$$

Where γ is the ratio of specific heats, $(dP/dt)_{max}$ is the peak PRR, P_{max} is the maximum of in-cylinder pressure, R is the ideal gas constant, and T_{max} is the maximum of in-cylinder temperature.

Analysis of mixing process

A 1-D in-house developed spray model DICOM is used to estimate equivalence ratio distributions in the fuel jet in order to get better insight into the variations in mixture distribution associated with the variations in the parameters studied in the experimental tests. The start of combustion and the combustion development have an extreme dependency on the local mixture conditions at Start of Spark (SoS) timing. The inputs of the DICOM model are the in-cylinder thermodynamic conditions (pressure, temperature and density), the spray cone angle, the fuel mass flow rate and the spray momentum. The model solves the general conservation equations either in a transient or steady state formulation for axial momentum and fuel mass along the center line. The results can be used to calculate values of spray velocity, species mass fractions and other values of the mixing process [29]. Finally, with some other assumptions described in [30], the model is used to obtain different temporal evolutions such as the spray liquid and vapor penetration, maximum spray velocity, equivalence ratio along the center line of the spray and the fuel mass fraction which has mixed to different equivalences ratios. The fuel mass fraction is the main variable used in this research.

Image processing tools

In order to complement the information about the differences in the combustion development for both injection strategies, time resolved parameters were calculated for every image in each sequence following a well-defined methodology. First, segmentation was performed for every image by calculating a threshold value, which is equal to the minimum digital level in the image plus 15% of the difference between the maximum and the minimum. This percentage was set, based on previous experience, as a compromise to remove light reflected off the liquid spray and the chamber walls without losing much information from the combustion event [31,32]. After segmentation, the flame area is defined as the summation of the number of pixels which belong to the flame (above the threshold). Thus, for every individual image, the digital levels of all pixels containing the combustion radiation (those above the threshold) are accumulated and averaged over the number of pixels of the flame area, obtaining an instantaneous parameter named I_{cummul} which represents a single mean flame intensity. Additionally, the integrated luminosity (IL) is defined as the integral of the instantaneous I_{cummul} along the whole cycle and luminosity delay (LD_{25}) as the time between the start of injection and the time where 25% of the integrated luminosity is registered.

Influence of Spark Assistance on Gasoline PPC

As stated in the introduction section, gasoline PPC has been confirmed as an adequate strategy to reduce emissions and improve thermal efficiency simultaneously, being their main drawbacks associated to the controllability and stability at light load operating conditions. This section is focused on evaluating the spark assistance as a possible solution to provide spatial and temporal control on gasoline PPC light load combustion. In order, to be able to assess the spatial control of the spark assistance, this study has been performed in the optical engine configuration. Thus, Figure 5 shows the parameters derived from the in-cylinder pressure signal analysis of 20 cycles with (down) and without (up) the use of the spark assistance. Specifically, IMEP, CA10, combustion duration (CA90-CA10) and the fuel energy conversion efficiency calculated from the RoHR versus the cycle number are presented. In addition, Figure 6 shows the parameters derived from the natural luminosity images processing. The accumulated intensity and the luminosity delay are presented versus the cycle number in order to compare, by means of natural luminosity images, the stability a controllability obtained with and without the use of the spark assistance. The spark plug discharge is also depicted in the figure. The engine operating conditions investigated in this study are shown in Table 4.

Table 4. Engine operating conditions set to evaluate the influence of the spark assistance on gasoline PPC.

Engine speed	750 rpm
Intake Temperature	343 K
Intake Pressure	1.6 bar
Exhaust Pressure	1.8 bar
Intake XO_2	18%
Injection Pressure	600 bar
SoI	-19 CAD
SoS	EoI
Fuel mass	18 mg/cc

As it can be appreciated in the IMEP and CA10 values from the PPC tests shown in Figure 5 (up), high cycle-to-cycle variation is obtained in this low load. It is interesting to note that due to the lean global equivalence ratio in this tests (ϕ=0.37) some tests present near zero IMEP due to the non-progression of the combustion event, resulting in an unacceptable coefficient of variation values. Moreover, the fuel energy conversion efficiency attained in the cases in which the combustion is achieved are extremely low (below 70%), expecting a considerable amount of CO and unburned HC emissions in these conditions. The combustion duration is around 4 ms in all the cases. By contrast, in Figure 5 (down) it is possible to appreciate that by means of the use of the spark assistance a controlled combustion is achieved in all the cycles. In spite of the lean global equivalence ratio (ϕ=0.37), the equivalence ratio stratification provided by the injection event allows in-cylinder regions with enough richer equivalence ratios to initiate the combustion if an external source of energy is added. Thus, the start of the spark discharge (SoS) must be set in the proper instant to initiate the combustion. If the SoS is set during the injection event, excessive rich equivalence ratios are found promoting the soot formation during the premixed flame propagation. By contrast, if the start of spark is set after the end of injection, excessive lean equivalence ratios are achieved leading a misfiring as the PPC cases. Thus, considering the gasoline direct injection literature [33], the spark discharge is set at the end of the injection in all cases in order operate within the “ignitability window” range. To illustrate the three situations commented above, Figure 4

shows the fuel mass distribution calculated by means of the 1D spray model between the spark plug electrodes for three different instants in the cycle (SoS<EoI, SoS=EoI and SoS>EoI).

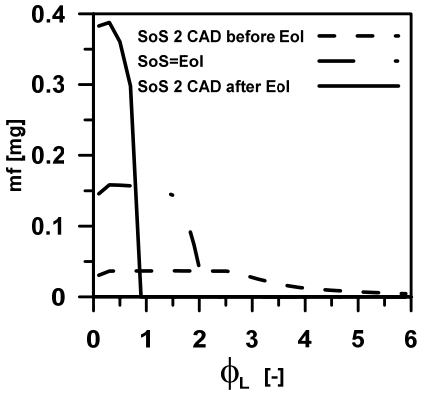

Figure 4. Fuel mass distribution between the spark plug electrodes for three different instants during the combustion cycle (2 CAD before the EoI, just at EoI and 2 CAD after the EoI).

From Figure 5, a noticeable improvement in the FeCE is observed with stable IMEP values (CoV IMEP below 4.5%) when using the spark assistance. Focusing on the CA10 values it is possible to state that the time from the start of spark (which corresponds to SOC) to CA10 is almost equal in all cycles. Thus, it is demonstrated that the spark assistance is promoting and controlling the combustion development in cases in which without the use of the spark plug no combustion (or not stable) is attained. It is interesting to note that due to the introduction of a spark plug to initiate the combustion, a larger combustion duration (around 0.5 ms) is observed compared to the autoignition achieved when a proper in-cylinder conditions are attained in the PPC tests.

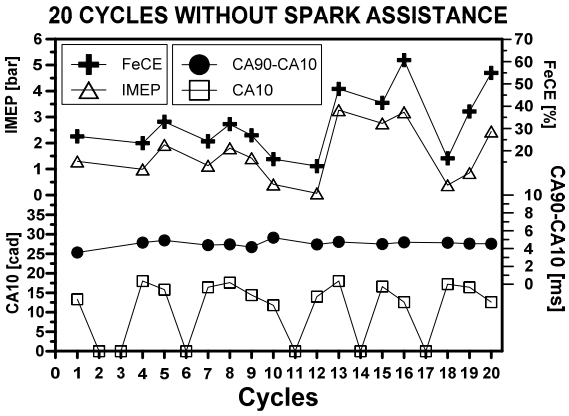

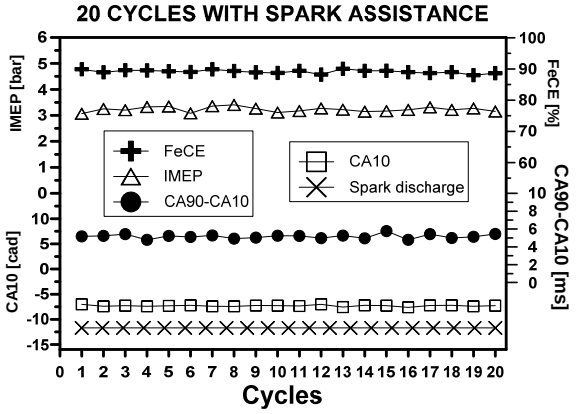

Figure 5. Combustion parameters derived from the in-cylinder pressure signal analysis. 20 cycles without spark assistance (up) and 20 cycles with spark assistance (down).

The comparison of the parameters derived from the processing of the natural luminosity images presented in Figure 6 also confirm the potential of the spark assistance. The accumulated intensity, due to it is an integrated parameter along the whole engine cycle, it is useful as a tracer of the combustion stability. On the other hand, luminosity delay allows to corroborate the CA10 results obtained by means of the in-cylinder pressure signal analysis. Comparing both batch of tests (without spark plug versus with spark plug) it is possible to appreciate that the accumulated intensity registered by using the spark assistance has better cycle-to-cycle stability, which manifest a more similar combustion development compared with the PPC tests. Also of note are the higher accumulated intensity levels obtained with the use of the spark plug, which are associated to the richer local equivalence ratios and higher temperatures achieved during the combustion event. Regarding the luminosity delay, it is almost constant for the 20 cycles using the spark. In addition, longer luminosity delays are registered without the use of the spark assistance due to the slowing down in the combustion development as a consequence of the lean global equivalence ratio.

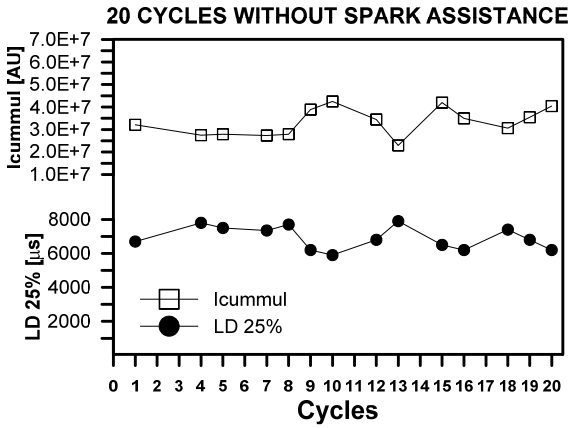

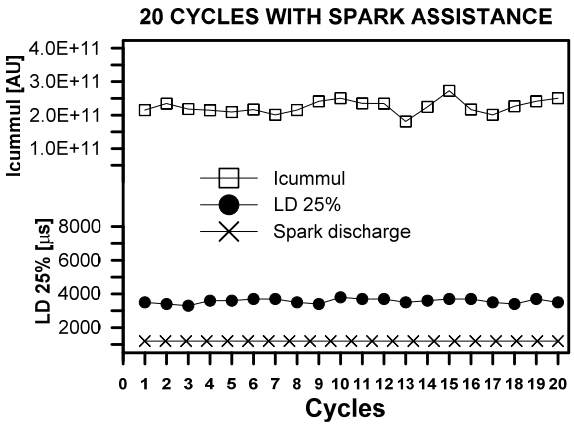

Figure 6. Combustion parameters derived from the natural luminosity images processing. 20 cycles without spark assistance (up) and 20 cycles with spark assistance (down).

Finally, in order to assess the spatial control provided by the spark assistance, Figure 7 shows a scheme of the combustion chamber in which the location of the first luminosity combustion spot registered after the spark discharge for the different combustion cycles with and without spark assistance are shown. All the spark assisted cycles are confined in a region near the spark plug location. Recall that the spots are slightly displaced from the center of the spark plug due to the effect of the swirl motion. By contrast, a high dispersion is observed comparing between the PPC cycles.

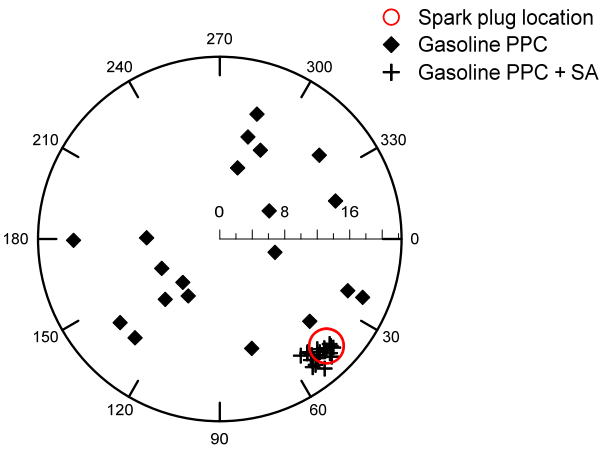

Figure 7. In-chamber location of the first combustion luminosity spot for different combustion cycles with and without spark assistance. In the cases with SA the first luminosity spot is registered after the spark discharge.

With the aim of evaluating the spark assistance effect on gasoline PPC in a higher load range, Figure 8 presents the coefficient of variation of IMEP and the ignition delay (CA10-EoI) versus load for 200 engine cycles with and without spark assistance. In addition, the combustion duration metric CA90-CA10 has been included for the higher and lower loads for both scenarios (PPC with and without spark assistance). The sweep has been carried out by keeping constant the engine settings presented in Table 4 and increasing progressively the injected fuel mass. Note that the EoI-CA10 value is presented every 0.5 bar with their mean value and their deviation bars.

Considering the results, it is clear that the use of the spark plug provides higher stability with a noticeable reduction of CoV IMEP from the lowest load to 5 bar and a slight improvement from 5 to 8 bar. Regarding the controllability, the almost constant trend of the ignition delay for the tests with spark assistance and their small deviation bars confirms the great controllability that the spark provides, being the ignition delay almost unaffected by the load (and the different in-cylinder conditions). As expected, without the use of spark assistance, lower ignition delays are achieved as the load is increase with minor deviation.

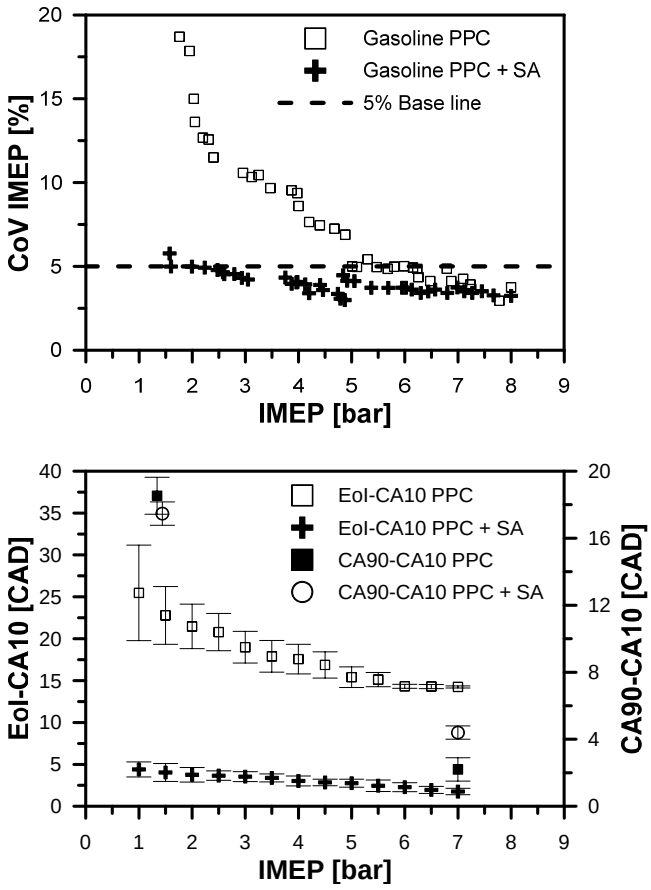

Figure 8. Coefficient of variation of IMEP (up) and ignition delay (CA10-EoI) versus load (down) for 200 engine cycles with and without spark assistance.

Focusing on the combustion duration, estimated by the CA90-CA10 combustion metric in Figure 8, it is possible to note two clear effects. On one hand, as the load is increased the combustion duration is shortened whether the spark assistance is used or not. This trend is explained due to the fact that under low load conditions (with lean equivalences ratios) the combustion development turns more unstable (as the values of CoV IMEP show). On the other hand, it is interesting to note that the effect of the spark assistance is different comparing the lower and higher loads. At high loads, where the in-cylinder conditions are proper to promote a stable autoignition of the mixture, the use of the spark assistance slows down the combustion development making that some fuel amount burns as a flame propagation instead of an autoigniton (faster than the flame propagation). At low loads, where the in-cylinder conditions are more adverse to achieve a stable combustion,

the energy addition by means of the spark plug provides better stability making the combustion development slightly faster. Also of note are the smaller error bars for the tests with spark assistance, which also confirms the improvement achieved in terms of stability.

As noted in the introduction section, another limitation of the PPC combustion mode but in this case at high loads is the knocking level. Figure 9 presents the ringing intensity, as a tracer of knocking level, versus load for 200 engine cycles with and without spark assistance. At very low loads the knocking level is similar for the cases with and without spark assistance (note that even with similar knocking levels the difference in the combustion efficiency is noticeable comparing this cases). As the load is increased, the ringing intensity reduction in the spark assisted cases is remarkable. As demonstrated in Figure 5 the use of the spark plug to initiate the combustion results in a longer combustion duration. Due to the combustion event is initiated by a spark plug before achieving the favorable in-cylinder conditions to allow an autoignition some fuel amount is consumed. Thus, the lower amount of fuel available at autoignition time results in a reduction of the maximum in-cylinder pressure peaks.

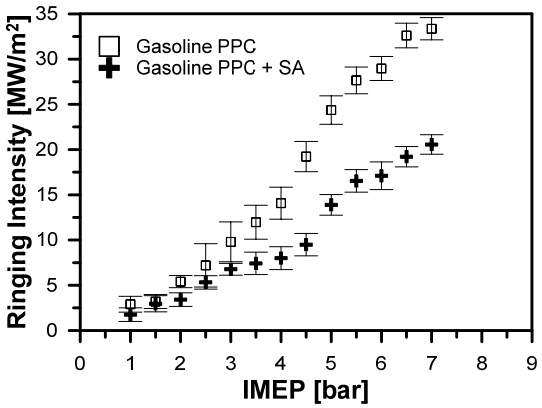

Figure 9. Ringing intensity versus load for 200 engine cycles with and without spark assistance.

Benefits of Double Injection on Gasoline PPC with Spark Assistance

In order to assess the benefits of using double injection strategies in the gasoline PPC with spark assistance combustion mode, a single injection reference case was selected based on author's previous work [34]. Specifically, a merit function [35] was used to select the proper engine operating condition taking into account some constraints; EURO VI limits for pollutant emissions and knocking level below 20 MW/m^2. The contribution to the merit function from a given variable will be zero if only the measured value is less than or equal to the specified limit. When F is non-zero, the contribution from each constrained parameter can be examined separately to quantify the severity of its non-compliance. The merit function is defined as follows (5):

$$F = \sum_i max\left(0, \frac{x_i}{x_i^*} - 1\right) \quad (5)$$

Where F is the merit function, x_i is the value of the i^{th} constrained parameter at the given conditions, x_i^* is the constraint of the i^{th} parameter and i is the index over all of the constraints.

The selected single injection test from the application of the merit function was obtained with an injection pressure of 900 bar, intake XO_2 of 19.6% and injected fuel mass of 21 mg/stk. Additionally, the injection timing was located at -9 CAD ATDC leading a combustion development close to the expansion stroke, which imply a combustion development under lower combustion temperatures minimizing the NOx emission levels. As commented above, the spark discharge was set at the end of the injection event. Based on these operating conditions, different double injections strategies was tested by sweeping the pilot injection timing and the intake XO_2. In all the cases, the fuel mass was split 50% in each injection. Moreover, the end of the main injection was set at the same instant than the single injection (corresponding with SoI_{main}=-7.5 CAD ATDC) and the spark discharge was set at the end of the main injection. Thus, the spark timing is equal in both strategies. Every other parameter was fixed from the single injection reference case conditions. Table 5 summarizes the engine operating conditions investigated in this study.

Table 5. Engine operating conditions set to study the benefits of the double injection on gasoline PP with spark assistance.

	Single inj.	Double inj.
Engine speed	1000 rpm	
Intake Temperature	343 K	
Intake Pressure	1.6 bar	
Exhaust Pressure	1.8 bar	
Intake XO_2	19.6%	19.6% to 17%
Injection Pressure	900 bar	
Inj. timing	-9 CAD	pilot:-31 to -12 CAD main=-7.5 CAD
Start of Spark	EoI	EoI_{main}
Fuel mass	21 mg/cc	

In order to compare both injection strategies, the merit function was applied to all the double injection tests using in this case as a constraints the engine-out emissions, ringing intensity and IMEP values of the single injection reference test. The results are presented in Figure 10. As it is possible to see, the XO_2 reduction worsens the merit function (higher values). Moreover, as the pilot injection timing is advanced this effect is more noticeable. It should be related with the lean global equivalence ratio (ϕ=0.4) used in this study. On this regard, for these operating conditions the increase in the dwell between the two injection events can promote an overmixing, which is magnified with the reduction in the intake oxygen concentration. Focusing on the detailed view from -16 to -19 CAD ATDC it is clear that the higher oxygen concentration tested (XO_2=19.6%) allows better results, and specifically the pilot injection timing of -16 CAD ATDC leads merit function

values near zero. Based on this findings, the selected double injection strategy was -16/-9 CAD ATDC.

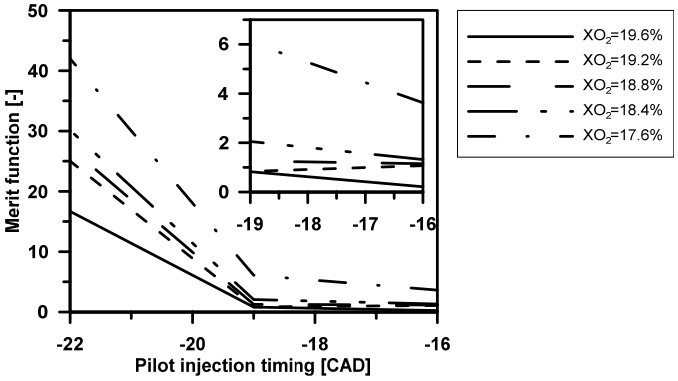

Figure 10. Merit function results for a double injection strategy sweeping the pilot injection timing and the intake oxygen concentration.

Figure 11 presents the results in terms of soot, NOx, unburned HC and CO for the single injection reference case and the best results obtained from the double injection sweep. Recall that the present study was carried out without any optimization in terms of engine hardware or settings. In addition, IMEP and combustion efficiency are shown in Figure 12. As it can be stated in Figure 11 the double injection strategy provides a great improvement in terms of unburned HC and CO emissions in comparison to the single injection strategy, which combined improvement is registered in the combustion efficiency (93% versus 88%). By contrast, higher NOx levels are registered in the case of the double injection strategy with almost constant soot levels. In addition, a benefit around 18% in the IMEP is achieved.

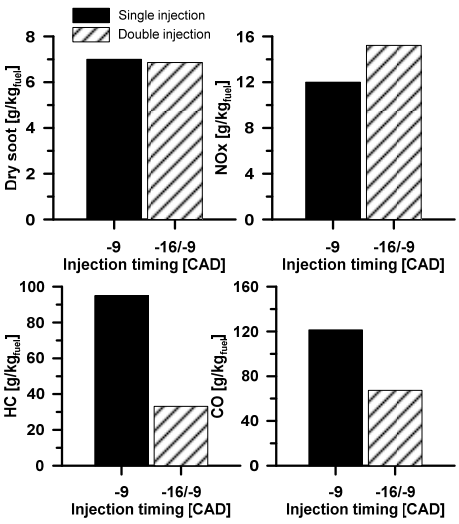

Figure 11. Dry soot, NOx, unburned HC and CO from the gasoline PPC combustion using a single (-9 CAD) and double (-16/-9 CAD) injection strategy.

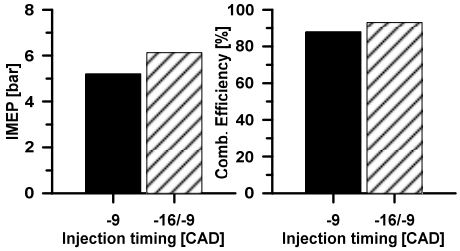

Figure 12. IMEP and combustion efficiency from the gasoline PPC combustion using a single (-9 CAD) and double (-16/-9 CAD) injection strategy.

Combustion development discussion

With the aim of understanding the differences found comparing the engine-out emissions between the single and double injection, this section analyzes the combustion development combining the analysis of the pressure signal, the results from the 1D spray model and the in-cylinder images acquired from the optical engine configuration. Figure 14 shows the crank angle evolution of the fuel mass flow rate and the rate of heat release for the two cases compared above (single injection: -9 CAD ATDC and double injection: -16/-9 CAD ATDC). In addition, natural luminosity (NL) and OH radical images in the key instants of the cycle are presented. The crank angle degree, in-cylinder pressure and unburned temperature corresponding with each image are showed above them. In addition, the spark plug location (SP) and the swirl motion are represented in the first image.

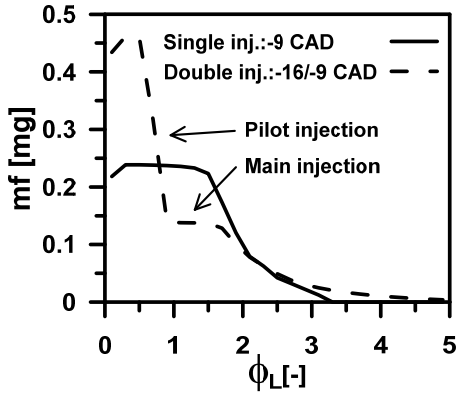

Figure 13. Fuel mass distribution between the spark plug electrodes for the single (-9 CAD ATDC) and double (-16/-9 CAD ATDC) injection strategies at the time of Start of Spark discharge (SoS).

Looking at the first NL images of the combustion cycle at -2.8 CAD ATDC, just after the spark discharge, it is observed a first kernel near the spark plug which presents intensity values above the minimum threshold of the correlated color scale. Comparing the intensity values for the single and double injection strategies according to the intensity scale, it is possible to state that higher luminosity is registered in the case of the single injection. The luminosity is well related with the equivalence ratios distribution near the spark plug location when the energy is released between the electrodes. In this sense, Figure 13 presents the fuel mass distribution between the spark plug electrodes for the two injection strategies studied. Two zones are identified for the double injection

strategy at the time of SOC (dashed trace). The first zone containing the mixture below stoichiometric equivalence ratio ($0.2<\phi<0.7$) is attributed to the pilot injection, which has had enough mixing time to reach a leaner mixture distribution. The second zone, with equivalence ratio ($\phi>0.7$) is attributed to the extra fuel mass provided by the main injection. As it is possible to appreciate, the local conditions near stoichiometric needed to ignite the mixture with the spark plug are achieved by the fuel mass injected in the main injection. This leaner equivalence ratio distribution obtained with the double injection strategy results in a fainter kernel near the spark plug. The lean local equivalence ratios for the double injection leads also to a lower in-cylinder temperature, as it is confirmed comparing OH images at this time (-2.8 CAD ATDC) for both injection strategies.

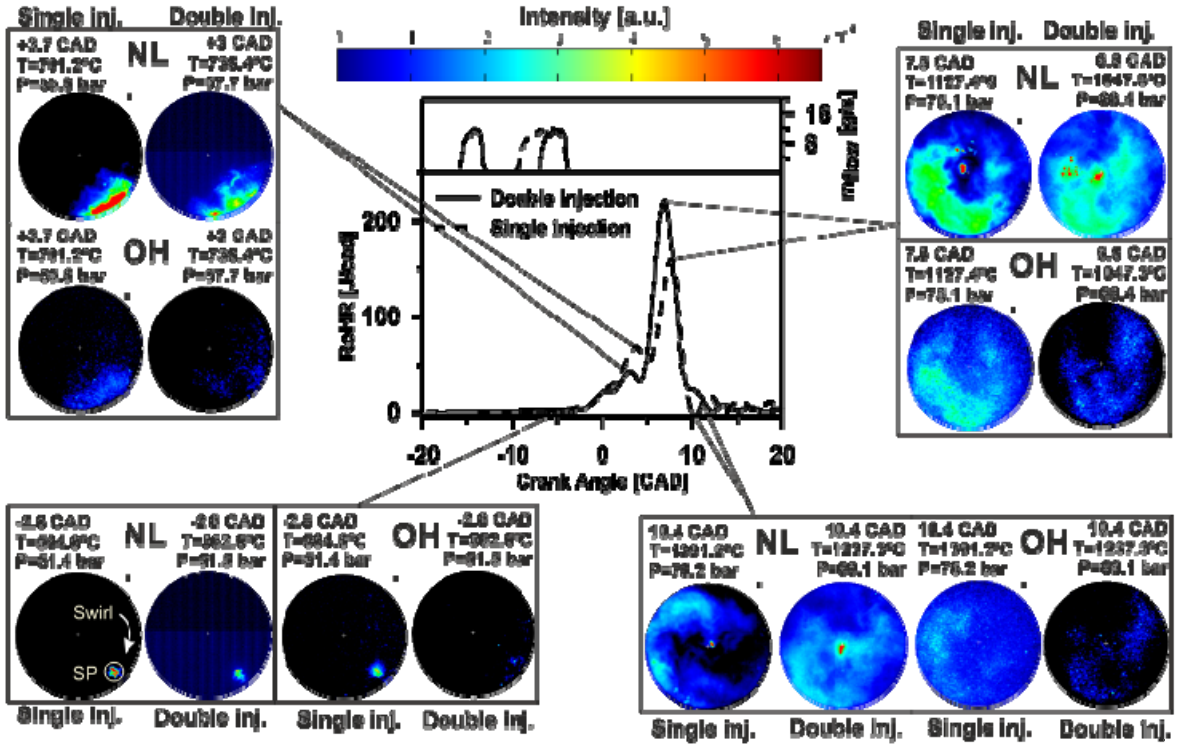

Figure 14. Fuel mass flow rate and RoHR crank angle evolution for the single injection: -9 CAD ATDC and double injection: -16/-9 CAD ATDC strategies.

A premixed flame is generated after the spark discharge, which leads to a first growth in the RoHR achieving its maximum at +3.7 CAD ATDC and +3 CAD ATDC in the case of the single and double injection, respectively. The higher local equivalence ratios of the single injection strategy leads a higher maximum in the RoHR profile. In addition, a greater intensity is registered for this injection strategy comparing the pair of NL and OH images at this time. After the increase in the pressure and unburned gas temperature as a consequence of the premixed flame evolution, an autoignition of the rest of the mixture is attained. In this case, the double injection strategy results in a higher maximum RoHR as the comparison of both profiles reveals, which causes a higher in-cylinder pressure and temperature. This fact is explained due to the more homogeneous mixture distribution achieved by means of the pilot injection as well as the higher fuel amount available (lower fuel mass burnt during the premixed flame evolution). Finally, the extinction of the flame at +10.4 CAD ATDC approximately with a late burning is observed in both cases. Once again, the area covered by the flame is clearly higher in the case of the double injection strategy.

Conclusions

The current study demonstrated the impact of the spark assistance and double injection strategy on the gasoline PPC combustion concept fuelled with high ON gasoline combining theoretical and practical tools. Specifically, an analysis of the parameters derived from in-cylinder pressure measurement has been combined with the 1-D spray model calculations. In addition, images of the natural luminosity and OH radical as well as different parameters derived from these images have been also analyzed.

From the study of the impact of the spark assistance on gasoline PPC, the conclusions can be drawn as follows:

-The start of the spark discharge (SoS) must be set in the proper instant to initiate the combustion. Excessive rich or lean equivalence ratios are found if the SoS is set during the injection event or after the end of injection, respectively.

-The spark assistance provides spatial control over the combustion process. The combustion development in all the spark assisted tests is clearly initiated in a region near the spark plug location.

-The constant values of CA10-SoS assess the temporal control provided by the spark assistance. This behavior is also found considering the in-cylinder images. Thus, the comparison of the CA10 and luminosity delay (LD25) confirms the great controllability that the spark provides comparing to the gasoline PPC combustion mode.

-The comparison of the IMEP and cumulated luminosity reveals that the spark assistance enhances the cycle to cycle repeatability in the gasoline PPC mode under low-medium load conditions.

-The spark assistance usage extends the PPC stable operating window under low load conditions. Thus, a significant reduction of the CoV IMEP in the region from 1.5 to 3 bar IMEP is achieved. Specifically, an almost constant value of 5% CoV IMEP is reached in the spark assisted cases, while values from 10% to 18% are registered in the PPC tests.

-The spark assistance allows a reduction in the ringing intensity by consuming part of the charge during the premixed flame growth. As the load is increased the reduction is more remarkable.

The notable observations comparing single and double injection strategies were as follows:

-The double injection strategy provides a great improvement in terms of unburned HC and CO emissions in comparison with the single injection strategy, which combined improvement is registered in the combustion efficiency (93% versus 88%). By contrast, higher NOx levels are registered in the case of the double injection strategy with almost constant soot levels. In addition, a benefit around 18% in the IMEP is achieved.

-The improvement in the spatial mixture distribution with double injection enhances the region in which the combustion takes place covering the whole combustion chamber, as the in-cylinder images demonstrate. Thus, in spite of having a leaner equivalence ratio distribution, a reduction in the incomplete combustion is achieved. The leaner equivalence ratios result in a lower intensity of the luminosity registered, however, the higher amount of fuel available to burn during autoigntion leads an increase in the in-cylinder temperature providing also a slight increase in NOx emissions.

Finally, it is important to remark that the present work was carried out without any optimization in terms of engine hardware settings and consequently more research is needed to found the optimum conditions.

References

1. Yanagihara, H., Sato, Y., Minuta, J., “A simultaneous reduction in NOx and soot in diesel engines under a new combustion system (Uniform Bulky Combustion System e UNIBUS)”, 17th International Vienna Motor Symposium, pp. 303-314, 1996.
2. Wu, H-W., Wang, R-H., Ou, D-J., Chen, Y-C., Chen, T-Y., “Reduction of smoke and nitrogen oxides of a partial HCCI engine using premixed gasoline and ethanol with air,” Applied Energy, Vol. 88, pp 3882-3890, 2011.
3. Akagawa, H., Miyamoto, T., Harada, A., Sasaki, S., et al., “Approaches to Solve Problems of the Premixed Lean Diesel Combustion,” SAE Technical Paper 1999- 01-0183, 1999.
4. Kimura, S., Aoki, S., Kitahara, Y., Aiyoshizawa, E., “Ultra-clean Combustion Technology Combining a Low-temperature and Premixed Combustion Concept for Meeting Future Emission Standards,” SAE International, SAE 2001-01-0200, 2001.
5. Maurya, R.K., Agarwal, A.K., “Experimental study of combustion and emission characteristics of ethanol fuelled port injected homogeneous charge compression ignition (HCCI) combustion engine,” Applied Energy, Vol. 88, pp 1169-1180, 2011.
6. Lu, X., Han, D., Huang, Z., “Fuel design and management for the control of advanced compression-ignition combustion modes,” Progress in Energy and Combustion Science, 37, 2011:741-783.
7. Mingfa, Y., Zhaolei, Z., Haifeng, L., “Progress and recent trends in homogeneous charge compression ignition (HCCI) engines,” Progress in Energy and Combustion Science 35 (5) (October 2009) 398-437.
8. Cerit, M., Soyhan, H.S., “Thermal analysis of a combustion chamber surrounded by deposits in an HCCI engine,” Applied Thermal Engineering 50 (1) (2013) 81-88.
9. Kiplimo, R., Tomita, E., Kawahara, N., Yokobe, S., “Effects of spray impingement, injection parameters, and EGR on the combustion and emission characteristics of a PCCI diesel engine,” Applied Thermal Engineering 37 (May 2012) 165-175.
10. Singh, A.P., Agarwal, A.K., “Combustion characteristics of diesel HCCI engine: an experimental investigation using external mixture formation technique,” Applied Energy 2012.
11. Law, D., Kemp, D., Allen, J., Kirkpatrick, G., Copland, T., “Controlled combustion in an IC-engine with a fully variable valve train,” SAE paper 2001-01-0251; 2001.
12. Agrell, F., Ångström, H.E., Eriksson, B., Wikander, J., Linderyd, J., “Integrated simulation and engine test of closed loop HCCI control by aid of variable valve timings,” SAE paper 2003-01-0748; 2003.
13. Haraldsson, G., Tunestål, P., Johansson, B., Hyvönen, J., “HCCI combustion phasing in a multi cylinder engine using variable compression ratio,” SAE paper 2002-01-2858; 2002.
14. Maurya, R.K., Agarwal, A.K., “Experimental investigation on the effect of intake air temperature and air–fuel ratio on cycle-to-cycle variations of HCCI combustion and performance parameters,” Applied Energy, Vol. 88, pp 1153-1163, 2011.
15. Yang, J., Culp, T., Kenney, T., “Development of a Gasoline Engine System Using HCCI Technology e the Concept and the Test Results,” SAE paper 2002-1-2832.

16. Kalghatgi, G.T., Kumara Gurubaran, R., Davenport, A., Harrison, A.J., Hardalupas, Y., Taylor, A.M.K.P., “Some advantages and challenges of running a Euro IV, V6 diesel engine on a gasoline fuel,” Fuel, Vol. 108, pp 197-207, 2013.
17. Yu, C., Wang, J., Wang, Z., Shuai, S., “Comparative study on Gasoline Homogeneous Charge Induced Ignition (HCII) by diesel and Gasoline/Diesel Blend Fuels (GDBF) combustion,” Fuel, Vol. 106, pp 470-447, 2013.
18. Lewander, C.M., Johansson, B., Tunestal, P., “Extending the Operating Region of Multi-Cylinder Partially Premixed Combustion using High Octane Number Fuel,” SAE Paper 2011-01-1394; 2011.
19. Weall, A., Collings, N., “Gasoline Fuelled Partially Premixed Compression Ignition in a Light Duty Multi Cylinder Engine: A Study of Low Load and Low Speed Operation,” SAE Int. J. Engines 2(1):1574-1586, 2009.
20. Persson, H., Rémon, A., Hultqvist, A., Johansson, B., “Investigation of the Early Flame Development in Spark Assisted HCCI Combustion Using High Speed Chemiluminescence Imaging,” SAE 2007-01-0212.
21. Persson, H., Rémon, A., Johansson, B., “The Effect of Swirl on Spark Assisted Compression Ignition (SACI),” JSAE 20077167, SAE 2007-01-1856; 2007.
22. Wang, Z., Shuai, S.J., Wang, J.X., Tian, G-H., Ma Xinliang Q.J., “Study of the effect of spark ignition on gasoline HCCI combustion,” Proceedings of the Institution of Mechanical Engineers, Part D: Journal of Automobile Engineering. http://dx.doi.org/10.1243/09544070JAUTO151.
23. Natajaran, V.K., Volker, S., Reuus, D.L., Silvas, G., “Effect of sparkignition on combustion periods during spark assisted compression ignition,” Combust Sci Technol 2009;181:1187–206.
24. Piock, W.F., Weyand, P., Wolf, E., Heise, V., “Ignition Systems for Spray-Guided Stratified Combustion,” SAE 2010-01-0598, 2010.
25. Payri, R., Novella, R., Garcia, A., Domenech, V., “A New Methodology to Evaluate Engine Ignition Systems in High Density Conditions,” Experimental Techniques 38 (2014) 17-28.
26. Benajes, J., García, A., Domenech, V., Durrett, R., “An investigation of partially premixed compression ignition combustion using gasoline and spark assistance,” Applied Thermal Engineering Vol 52 p. 468–477; 2013.
27. Lapuerta, M., Armas, O., Hernández, J.J., “Diagnostic of D.I. Diesel Combustion from In-Cylinder Pressure Signal by Estimation of Mean Thermodynamic Properties of the Gas.,” Applied Thermal Engineering. Vol 19 Nº 5 p. 513–529; 1999.
28. Eng, J., “Characterization of pressure waves in HCCI combustion,” SAE paper 2002-01-2859, 2002.
29. Pastor, J.V., López, J.J., García, J.M., Pastor, J.M., “A 1D model for the description of mixing-controlled inert diesel sprays,” SAE paper 2005-01-1126; 2005.
30. Desantes, J.M., Pastor, J.V., García-Oliver, J.M., Pastor, J.M., “A 1D model for the description of mixing-controlled reacting diesel sprays,” Combustion and Flame 2009; 156:234–49.
31. Pastor, J.V., Bermúdez, V., García-Oliver, J.M., Ramírez-Hernández, J.G., “Influence of spray-glow plug configuration on cold start combustion for high-speed direct injection diesel engines,” Energy 36 (2011) 5486-5496.
32. Pastor, J.V., García-Oliver, J.M., Pastor, J.M., Ramírez-Hernández, J.G., “Ignition and combustion development for high speed direct injection diesel engines under low temperature cold start conditions,” Fuel 90 (2011) 1556–1566.
33. Arcoumanis, C., Kamimoto, T., “Flow and combustion in reciprocating engines,” Springer, 2009.
34. Desantes, J.M., Payri, R., García, A., Monsalve-Serrano, J., “Evaluation of Emissions and Performances from Partially Premixed Compression Ignition Combustion using Gasoline and Spark Assistance,” SAE paper 2013-01-1664; 2013.
35. Cheng, A., Upatnieks, A., Mueller, C., “Investigation of Fuel Effects on Dilute, Mixing-Controlled Combustion in an Optical Direct-Injection Diesel Engine,” Energy Fuels, 21 (4), pp 1989–2002, 2007.

Contact Information

Corresponding author: Dr. Antonio García
angarma8@mot.upv.es

Definitions/Abbreviations

ASTM	America Society of Testing Materials
ATDC	After Top Dead Center
BMEP	Brake Mean Effective Pressure
CAD	Crank Angle Degree
CAI	Compression Autoignition
CI	Compression Ignition
CMOS	Complementary Metal Oxide Semiconductor
CoV	Coefficient of Variation
CA10	Crank Angle at 10% mass fraction burned
CA50	Crank Angle at 50% mass fraction burned
CA90	Crank Angle at 90% mass fraction burned
DI	Direct Injection
EGR	Exhaust Gas Recirculation
EOI	End of injection
EOI_{main}	End of main injection
EVO	Exhaust Valve Opening
FeCE	Fuel energy Conversion Efficiency

FFT	Fast Fourier Transform
FSN	Filter Smoke Number
HCCI	Homogeneous Charge Compression Ignition
IMEP	Indicated Mean Effective Pressure
IL	Integrated Luminosity
IVC	Intake Valve Closing
LTC	Low Temperature Combustion
LD	Luminosity Delay
NL	Natural luminosity
ON	Octane number
OH*	Hydroxyl radical
PFI	Port Fuel Injection
PID	Proportional-Integral-Derivative controller
PPC	Partially Premixed Charge
RoHR	Rate of Heat Release
RON	Research Octane Number
SP	Spark Plug
SI	Spark ignition
SoC	Start of Combustion
SOI_{main}	Start of main injection
SOI_{pilot}	Start of pilot injection
SoS	Start of Spark
TDC	Top Dead Center
UV	Ultraviolet
XO_2	Oxygen molar fraction